

# Green synthesis of silver, gold and silver-gold nanoparticles: Characterization, antimicrobial activity and cytotoxicity

Mostafa M.H. Khalil\*, D. Y. Sabry, Huda Mahdi

Chemistry Department, Faculty of Science, Ain Shams University, 11566, Abbassia, Cairo,  
Egypt  
Hudamahdi@gmail.com

## Abstract:

The present study reported a facile and rapid biosynthesis method for gold nanoparticles (GNPs) silver nanoparticles (AgNPs) and bimetallic heterogeneous silver-gold nanoparticles (AgAuNPs) using the leaves of *Gmelina arborea* (ROXB) (Family *Verbenaceae*) extract. The aqueous leaves extract was used as biotic reducing and stabilizing agent of the growing nanoparticles. The synthesized gold nanoparticles (AuNPs), silver nanoparticles (AgNPs) and silver-gold core-shell nanoparticles (AgAuNPs) were characterized using UV-Vis spectroscopy (UV-Vis), Fourier transform infrared spectroscopy, (FT-IR), X-ray diffraction (XRD), transmission electron microscopy (TEM) and thermal gravimetric analyses (TGA). Several factors such as the extract amount, contact time and solution pH, as possible influences; were investigated to obtain the optimized synthesis conditions. The antimicrobial activity study revealed that while the aqueous extract at concentrations of 0.8 and 4% (w/v) showed no effect on the antimicrobial activity, the produced nanoparticles, AuNPs, AgNPs and AgAuNPs inhibited the growth of Gram positive bacteria (*Bacillus subtilis*, *Staphylococcus aureus*), Gram negative bacteria (*E. Coli* and *Pseudomonas aeruginosa*) and Fungi (*Candida albicans* and *Aspergillus niger*). The cytotoxic activity against hepatocellular carcinoma (HePG2) was also evaluated.

## Keywords:

Biological synthesis; *Gmelina arborea*; gold nanoparticles; silver nanoparticles; silver-gold core-shell; nanoparticles, antibacterial activity; hepatocellular carcinoma

## 1. Introduction

Gold and silver nanoparticles are of great importance due to surface area and a high fraction of surface atoms. The scientific and technological implication of metal nanoparticles has made them the subject of intensive research. Both Ag and Au nanoparticles have been studied for biomedical applications of drug delivery, biomolecular recognition and molecular imaging (Sperling et al., 2008; Wilson, 2008).

Gold nanoparticles have been considered as an important area of research due to their unique and tunable surface plasmon resonance (SPR) and their applications in biomedical science including

tissue/tumor imaging, photothermal therapy and immuno-chromatographic identification of pathogens in clinical specimens (Huang,2006). Gold nanoparticles offered advantages of stability, low toxicity, facile tunability of AuNP size, and the possibility of functionalization of its surface(Lukianova-Hlebet al., 2012), therefore AuNPs can be successfully used in clinical diagnosis (Qin L.etal., 2017) cancer cell photothermolysis(Cho JHet al., 2017), bioimaging(Cho JHet al., 2017; Murphy C.Jet al.,2008) immunoassay(CederquistK.B. et al., 2017) and antimicrobial activity ( Pradeepa.K. et al., 2017)Since the development of the concept of green nanoparticle (Siddiqi K.S and Husen A, 2017),there is a growing the need for environmentally benign metal–nanoparticle synthesis processes that do not use toxic chemicals in the synthesis protocols to avoid adverse effects in medical applications. Biological synthesis especially using plant extract are available for the synthesis of AuNPs and involve reduction of gold cations ( $Au^+$  or  $Au^{3+}$ ) to zerovalent ( $Au^0$ ) with a reducing agent(Pradeepa K et al., 2017; Khalil M.M.H et al., 2012).

Silver NPs (AgNPs) are known to be the most effective against bacteria and viruses(S.Galdiero et al., 2011; Lara.H.H et al., 2010) In addition, microbes are unlikely to develop resistance against silver, because the metal attacks a broad range of target sites in the organisms(Pal S. et al.,2007). AgNPs target both the respiratory chain and the cell-division machinery, while concomitantly releasing silver ions ( $Ag^+$ ) that enhance bactericidal activity and finally leading to cell death(PrabhuS.and Poulouse EK,2012). The antimicrobial activity of AgNPs depends on their size(Lu.Z. et al., 2013) and shape(Furno F. et al., 2004). Diverse applications of AgNPs include wound dressings, coating for medical devices and surgical masks, woven fabric microfiltration membranes, and nanogels(Li Y. et al., 2006; AttaAM et al., 2014).

Green synthesis of stable AgNPs with controlled size and shape is a very profitable approach. As a result, some novel methods have recently been developed using microbes such as bacteria and fungi (Das VL et al., 2014; A. Syed et al., 2013) or plant extracts from seeds, leaves, and tubers(Jagtap U.Band Bapat VA ,2013;Ghosh S. et al., 2012) for the synthesis of AgNPs.The use of plants for AgNPs synthesis is preferred over other biological processes because there is noneed to grow microbes, less expensive and it could be suitably scaled up for large-scale NP synthesis. Plant extracts possess many antioxidants, which act as reducing as well as capping agents(MittalA.K et al., 2013).

Cancer is known to be the second leading cause of death in the world, so scientists attempt to discover harmless cancer therapy. In fact, most of the artificial agents being used currently in cancer therapy are toxic and can produce damage to the normal cells (Kampa M et al., 2000).Therefore, chemotherapy via nontoxic agents could be one solution for decreasing the risky effects of cancer.

*Gmelina arborea* (ROXB.) family *verbenaceae*(KaswalaR et al., 2012)having tremendous therapeutic potential that are not fully utilized. The leaves of *Gmelina arborea* have some important chemical constituents which are responsible for the medicinal significance of the

herb. The hexane extract of *Gmelina arborea* leaves exhibited vasorelaxant properties (Sylvie L.W et al., 2012). It contains a large concentration of alkaloids, luteolin as flavonoids as well as a variety of phytochemicals. The methanolic extract contains alkaloids, flavonoids, saponins, steroids, glycosides whereas chloroform extract contains alkaloids, saponins and steroids. So far, there is no report on the synthesis of nanoparticles using *Gmelina arborea* leaf extracts. In this paper, we report on the synthesis of silver, gold and their bimetallic nanoparticles using hot water *Gmelina* leaf extracts as a simple, low-cost and reproducible method.

## **2. Experimental**

### **2.1 Materials**

HAuCl<sub>4</sub>.H<sub>2</sub>O 99.9% and silver nitrate AgNO<sub>3</sub> were purchased from Aldrich. *Gmelina* leaves were collected from Botanical Garden of Orman- Giza (Egypt). A stock solution of HAuCl<sub>4</sub> was prepared by dissolving 1.0 g HAuCl<sub>4</sub>. H<sub>2</sub>O in 50 ml deionized water in a dark bottle. A stock solution of AgNO<sub>3</sub> (1 x 10<sup>-2</sup> M) was prepared by dissolving 0.084g in 50 ml de-ionized water. A 4.0g of *Gmelina* leaf broth was boiled for 15 min, filtered and completed to 100 ml to get the extract. Deionized water was used throughout the reactions. Hydrochloric acid, sulphuric acid and sodium hydroxide used for pH monitoring were also purchased from Sigma-Aldrich.

### **2.2. Characterization of the nanoparticles**

UV-visible spectra were recorded at room temperature using a Shimadzu 2600 spectrophotometer. X-ray diffraction (XRD) pattern was obtained using a Shimadzu XRD-6000 diffractometer with Cu K $\alpha$  ( $\lambda = 1.54056 \text{ \AA}$ ) to confirm the biosynthesis of nanoparticles. The size and morphology of the nanoparticles were examined and the TEM images were obtained on a JEOL-1200JEM for the TEM measurements. Fourier transform infrared (FTIR) spectra were recorded on a Nicolet 6700 FTIR spectrometer at room temperature. Thermogravimetric analyses were carried out with a heating rate of 10 °C/min using a Shimadzu DT-50 thermal analyzer.

### **2.3. Preparation of the aqueous extract**

4.0g of fresh leaves of *Gmelina* was washed with tap water, followed by distilled water, boiled for 15 min and the resulting extract was filtered through filter paper and completed to 100 ml with deionized water to get the (4% w/v) extract.

### **2.4. Synthesis of gold nanoparticles .**

For the synthesis of the gold nanoparticles, a certain volume of the *Gmelina arborea* leaves extract (4% w/v) was added to the 0.05 ml HAuCl<sub>4</sub>.H<sub>2</sub>O solution at room temperature and the volume was adjusted to 10 ml with deionized water. The final concentration of Au<sup>3+</sup> was 2.9 x 10<sup>-4</sup> M and the reduction process of Au<sup>3+</sup> to Au nanoparticles was followed by the change of the color of the solution from yellow to violet to dark pink and green depending on the extract concentration. For

the nanoparticles prepared at different pH values, the pH of the solutions was adjusted using 0.1 N HCl and 0.1 N NaOH solutions.

## 2.5. Synthesis of silver nanoparticles.

For the synthesis of the silver nanoparticles, 0.5 ml of the Gmelina leaf extract was added to the 0.1 ml  $\text{AgNO}_3$  solution and the volume was adjusted to 10 ml with de-ionized water. The final concentration of  $\text{Ag}^+$  was  $1 \times 10^{-4}$  M and the reduction process  $\text{Ag}^+$  to  $\text{Ag}^0$  nanoparticles was followed by the color change of the solution from yellow to brownish-yellow to deep brown within 24 hrs depending on studied parameters such as the extract concentration, time, temperature and pH. The pH of the solutions was adjusted using 0.1 N  $\text{H}_2\text{SO}_4$  and 0.1 N NaOH solutions.

## 2.6 Synthesis of AuAg bimetallic nanoparticles

For the synthesis of gold-silver nanoparticles, a 2.5 ml of plant extract (4g/ 100 ml deionized water) was added to 0.5 ml of  $\text{AgNO}_3$  solution  $1 \times 10^{-2}$  M and then after 24 hrs 0.05 ml of  $\text{HAuCl}_4$  solution  $5.8 \times 10^{-2}$  M was added at room temperature and the volume was adjusted to 10 ml. The final concentration of  $\text{Ag}^+$  was ( $5 \times 10^{-4}$  M) and the final concentration of  $\text{Au}^{3+}$  was  $2.9 \times 10^{-4}$  M and after 20 min reduction process was followed by the color change of the solution from brownish yellow to violet .

## 2.6. Cytotoxicity evaluation

*In vitro* anticancer activity evaluation of the nanoparticles was carried out against human cancer cell lines hepatocellular carcinoma (HePG2) using MTT method (Skehan P. et al., 1996) The relationship between drug concentrations and cell viability was plotted to calculate  $\text{LC}_{50}$ .

Potential cytotoxicity of the nanoparticles tested using cell line HePG2. Cells were plated in the 96-multiwell plate ( $10^4$  cells/well) for 24 hrs before treatment with the extract or nanoparticles to allow attachment of a cell to the wall of the plate. Triplicate wells were prepared for each individual dose. Monolayer cells were incubated with the compounds for 48 h at  $37^\circ\text{C}$  and atmosphere of 5%  $\text{CO}_2$ . After 48 h, 0.5% of the water-soluble mitochondrial dye 3-(4,5-dimethyl-2-thiazolyl)-2,5-diphenyl-2H-tetrazolium bromide ( $\text{MTT}^+$ ) was added. Incubation was continued for three more hours, the medium was removed and the water-insoluble blue formazan dye formed stoichiometrically from  $\text{MTT}^+$  was solubilized by acidic SDS. Optical densities were determined by a microplate reader (Tecan Infinite 200 Pro, Austria) at the wavelength of 570 nm. The relation between surviving fraction and drug concentration is plotted to get the survival curve of each tumor cell line after the specified compound.

## 2.7 Preparation of coated silver, gold and their bimetallic nanoparticles for antimicrobial assay

Two stock plant extracts (4% and 20% w/v) were prepared by boiling 4.0g and 20.0g of Gmelina leaves for 15 min, filtered and completed to 100 ml with deionized water. A 2 ml of the

extract solution (4% and 20% w/v) was used in the measurements and completed to 10 ml with deionized water. Different extract: Au<sup>3+</sup> and/or Ag<sup>+</sup> ratios were prepared by dilutions from stock solutions to obtain the samples denoted as group a, b, c, and d with final concentrations of the extract and the metal ions concentrations as follow: (a 1; 0.8% extract only), (a 2; 4% extract only), (b 2, 4% extract and 1.45X10<sup>-3</sup> M Au<sup>3+</sup>), (b 3 ; 4% extract and 2.9X10<sup>-3</sup>M Au<sup>3+</sup>) , (c 2; 4% extract and 5X10<sup>-4</sup> M Ag<sup>+</sup>), (c 3; 4% extract and 1X10<sup>-3</sup>M Ag<sup>+</sup>), (d 2; 4% extract and 1.45 X10<sup>-3</sup>M Au<sup>3+</sup> +2.5X10<sup>-3</sup>M Ag<sup>+</sup> ) and (d 3; 4% extract and 2.9 x10<sup>-3</sup>M Au<sup>3+</sup> +2.5x10<sup>-3</sup>MAg<sup>+</sup> )

## 2.8 Antimicrobial activity assay

The antimicrobial activity of the synthesized AuNPs, AgNps, and bimetallic nanoparticles was studied against the growth of Gram Positive bacteria (*Bacillus subtilis* ATCC 6633, *Staphylococcus aureus* ATCC 25923), Gram negative bacteria (*E. coli* ATCC 25922, *Salmonella typhimurium* and *Pseudomonas aeruginosa* ATCC 27858) and Fungi (*Candida albicans* ATCC 10231) in comparison with that of aqueous *Gmelina* leaf extract by using the standard agar well diffusion technique. The bacteria and fungi were maintained on nutrient agar medium and CzapeksDox agar medium, respectively. The agar media were inoculated with different microorganisms. After 24 h. of incubation at 30°C for bacteria and 48 h. of incubation at 28 °C for fungi, the diameter of inhibition zone (mm) was measured.

## 3 Results and discussion

### 3.1 UV–visible spectroscopy and TEM Studies

#### 3.1.1 Effect of concentration of *Gmelina* leaves extract

The primary variable in the reaction condition was the concentration of the *Gmelina* leaf extract. The formation and stability of gold nanoparticles were followed by UV-visible spectrophotometry. Figure 1 shows the UV-visible spectra of gold nanoparticles formation using constant HAuCl<sub>4</sub> concentration 2.9x 10<sup>-4</sup>M with different concentrations of extract from 0.2 to 3 ml. The inset shows photos of the color change of gold nanoparticles with changing the *Gmelina* leaves extract concentration. As is clear from the inset in Figure 1a the color changed from pale yellow to violet to dark pink and green depending on the extract concentration. As shown in Figure 1b, UV–vis spectra showed that in the range of low amounts of the leaf extract (0.2–2 ml in 10 ml solution), the absorption spectra exhibit a gradual increase of the absorbance accompanied with a shift in the λ<sub>max</sub> of SPR band absorption peak from 566 to 534 nm. With an increase in the quantity of extract, the full width at half maximum (FWHM) decreases supporting the reduction in particle size. Further addition of higher amounts of the extract, the λ<sub>max</sub> was shifted to longer wavelengths and the green color of the AuNPs solution was developed (inset of Fig. 1) with a slight decrease in absorbance (Khalil M.M.H. et al., 2014). This is most likely due to changes in the dielectric properties of the layer immediately surrounding the gold nanoparticles (Mulvaney P, 1996) and to some small amount of particle aggregation.

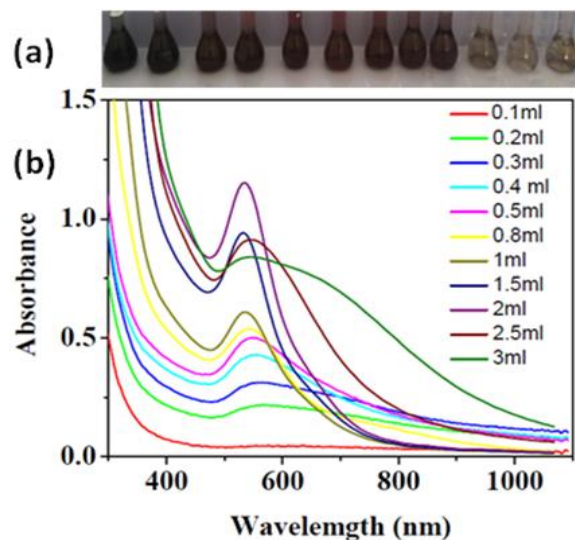


**Figure 1:** UV-Vis absorption spectra of (4% w/v) of the Gmelina leaf extract (a) The color change of gold solution formed using different concentrations of plant extract, (b) Uv-vis spectra of gold nanoparticles using constant  $\text{HAuCl}_4$  concentration  $2.9 \times 10^{-4} \text{M}$  with different concentrations of extract from 0.2 to 3 ml.

For silver nanoparticles prepared using Gmelina leaf extract, the SPR band of silver nanoparticles formed with different extract concentrations from 0.2 to 1.5 ml at room temperature after 24 hrs as there was no color developed within the first 2 or 3 hrs at room temperature. The color of the solutions changed from pale yellow to deep brown depending on the extract concentration. As the concentration of the Gmelina leaf extract increases, the absorption peak gets more sharpness and the blue shift was observed from 458 to 441 nm. The blue shifted and sharp narrow shape SPR band indicating the formation of a spherical and homogeneous distribution of silver nanoparticles was observed (Khalil M.M.H et al., 2014). It should be mentioned that the extract absorption has a maximum at about 400 nm and could contribute to the absorption of AgNPs at high extract concentration.

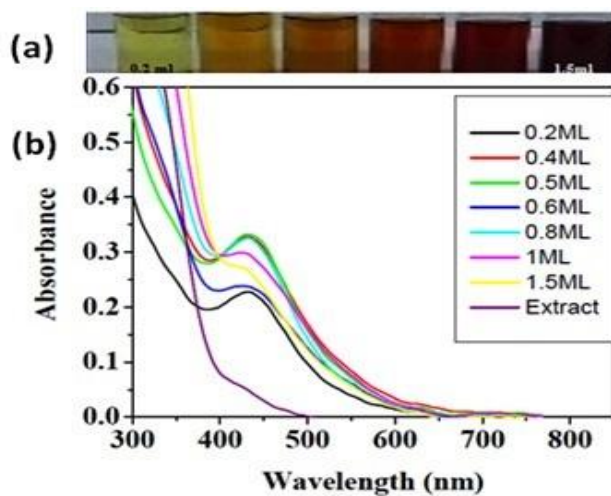


**Figure 2 :** (a) The color change of silver solution formed using different concentrations of Gmelina extract, (b) UV-vis spectra of silver nanoparticles using constant  $\text{AgNO}_3$  concentration ( $1 \times 10^{-4} \text{M}$ ) with different concentrations of extract from 0.2 to 1.5 ml.

Since the formation of AgNPs needs 24h at least for the reaction to finish, formation of AuAgNPs was carried out by addition of  $\text{AuCl}_4^-$  solution to the AgNPs using successive reduction process (Mallik K et al., 2001). AgNPs firstly prepared by adding 2.5 ml of plant extract (4%) to 0.5ml of silver nitrate ( $10^{-2}$  M), and left for 24hrs at room temperature to ensure formation of AgNPs, Fig 3, followed by addition of a 0.05ml of  $\text{AuCl}_4^-$  ( $5.8 \times 10^{-2}$  M) to the solution in Ag:Au 1:1 molar ratio. The UV–visible spectrum of the AuAgNPs exhibited a clear peak for the AuNPs while a band corresponding to silver nanoparticles is not observed using this concentration ratio. Similar spectra for the Au/Ag bimetallic solution using Neem leaf broth ( Shankar S.S et al., 2004) and Persimmon (*Diopyros kaki*) leaves (Song J. Yand Kim B.S, 2008) were observed and this can be attributed to the formation of gold nanoparticles layer formed a thin uniform film around the gold nanoparticles, leading to considerable damping of a distinct silver plasmon vibration band at ca. 430 nm and the surface plasmon absorption band showed only one peak which result from the metal of the shell. The damping of silver plasmon upon the formation of Au(Ag) nanoparticles could be also explained with the consideration of the standard reduction potential of  $\text{AuCl}_4^-/\text{Au}$  pair (0.99 V, vs SHE) which is higher than that of  $\text{Ag}^+/\text{Ag}$  pair (0.80 V, vs SHE), then silver nanoparticles can be oxidized by the addition  $\text{HAuCl}_4$  (Sun Y et al., 2002). Successive reduction is usually carried out to prepare “core-shell”-structured bimetallic nanoparticles (Mallik Ket al., 2001; Chen H.M et al., 2006). Previous studies have shown that co-mixed particle solutions contain two absorption maximums and not the presence of a single peak as was observed in our case.

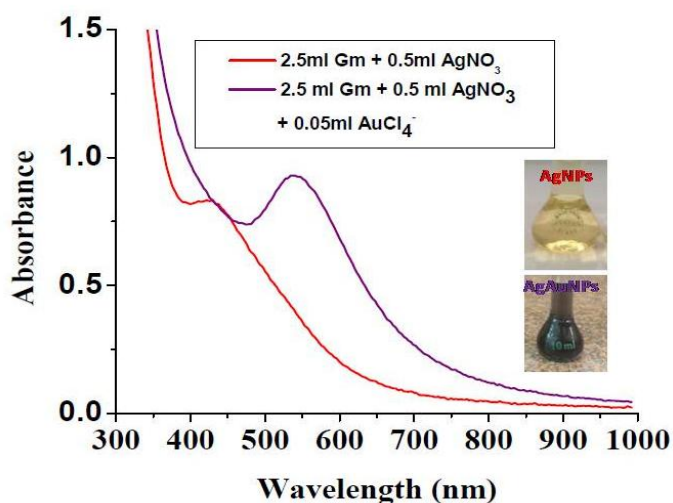


**Figure 3:** UV–Visible spectra of AgAu bimetallic nanoparticles 2.5 ml of plant extract (4%) was added to (0.5 ml) of silver nanoparticles using constant concentration ( $1 \times 10^{-2}$  M) and then after 24hrs (0.05 ) ml of gold nanoparticles using constant concentration ( $2.9 \times 10^{-4}$  M) was added at room temperature

The nanoparticles products were further characterized using Transmission Electron Microscopy (TEM). The TEM images confirm the formation of the nanoparticles, the gold

nanoparticles were spherical with an average size of 10 nm, Fig. 4(a), while the AgNPs were in the range of 70 nm and exhibited a range of different morphologies with irregular contours, Fig. 4(b). The core-shell silver-gold nanoparticles Au(Ag)NPs, Fig. 4(c) exhibit surface morphologies closed to AgNPs with obvious light portion for most nanoparticles supporting the formation of gold layer on AgNPs seeds. It can be seen that the size of AgAuNPs are smaller than AgNPs and that can be explained by the oxidation of AgNPs upon addition of  $\text{AuCl}_4^-$  before its reduction  $\text{Au}^0$  and form a layer on the AgNPs.

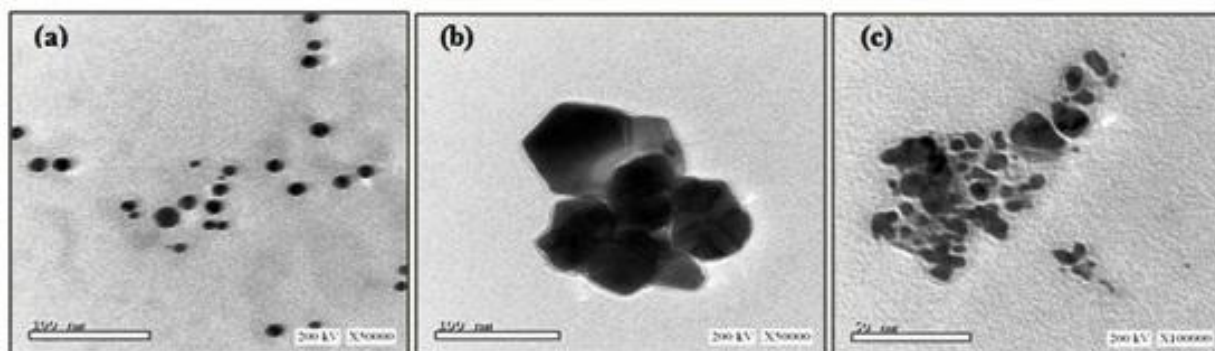
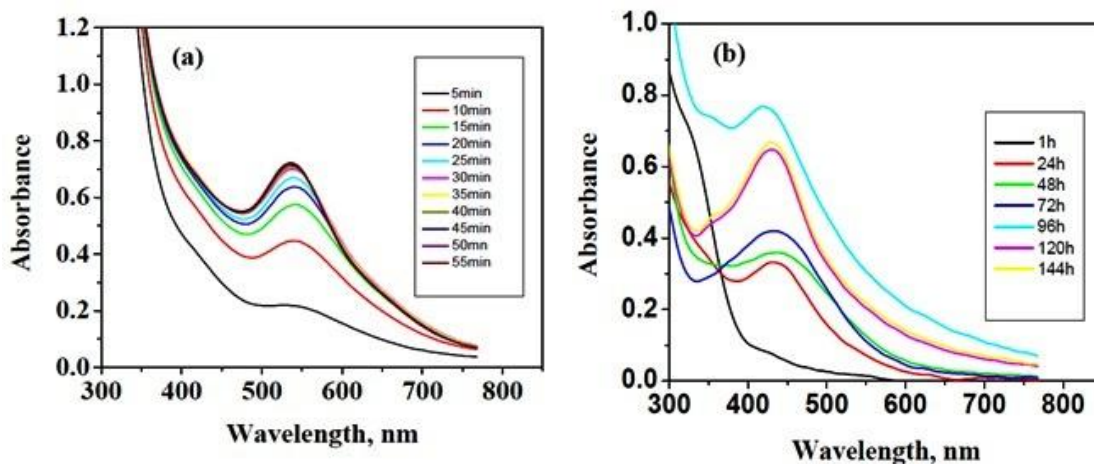


Figure.4. TEM images of (a) Au NPs.(b) AgNPs (c) AgAuNPs nanoparticles.

### 3.1.2 Effect of contact time

The effect of contact time between the  $\text{Au}^{3+}$  ions and  $\text{Ag}^+$  with the extract was studied at room temperature to follow the rate of reaction and the time necessary to complete the reduction process. Fig 5a shows the formation of AuNPs started within 5 min and increased with time. Absorption band showed no change after 35 minutes indicating the complete reduction of  $\text{Au}^{3+}$ . The reaction between  $\text{Ag}^+$  and the reducing material in the extract was followed for one week, Fig 5b. It can be seen that the absorption spectra and the color intensity of the solution increased with contact time and decreased slightly after 5 days. This result implies that the silver nanoparticles prepared by this green synthesis method is very stable without aggregation. It is pertinent to note that in previous studies the time span required for reduction of silver ions ranged from 24 to 48 h (Chandran S.P et al., 2006)





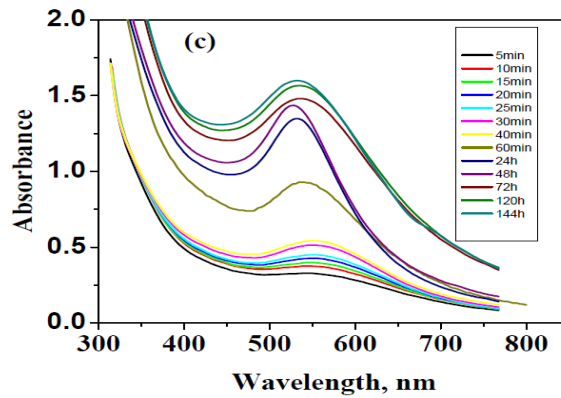
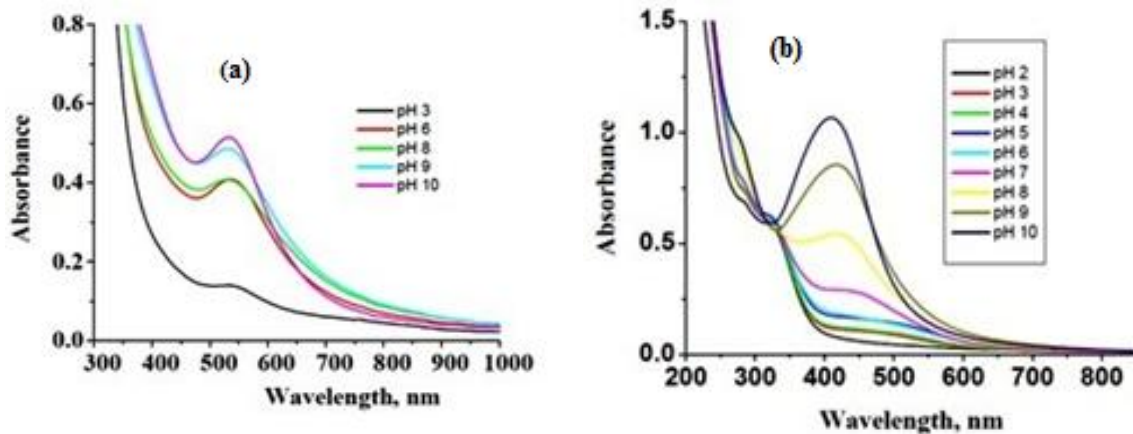


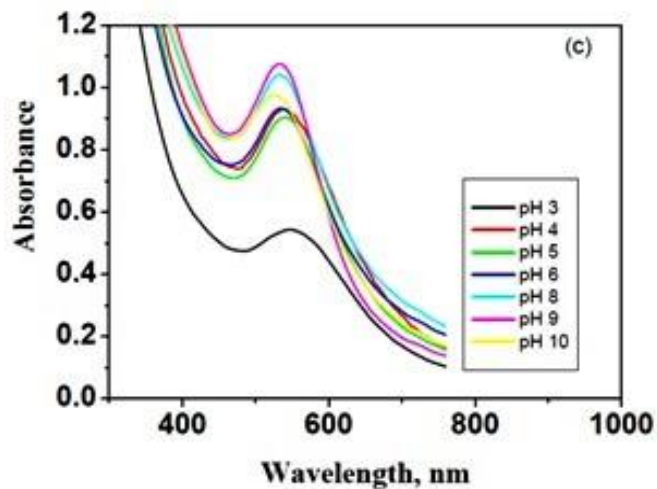
Figure 5: UV-visible spectra of (a) Au nanoparticles (b) Ag nanoparticles (c) AuAg nanoparticles, as a function of time at room temperature.

The rate of the Gmelina leaf extract mediated biosynthesis of AuAgNPs is studied by monitoring the absorption intensity of the SPR for 6 days. As shown in Fig.5c the bioreduction started within 60 min then increased dramatically and after 4 days there was nearly no change in the absorption intensity indicating that the reaction was completed within 4 days.

### 3.1.3. Effect of pH

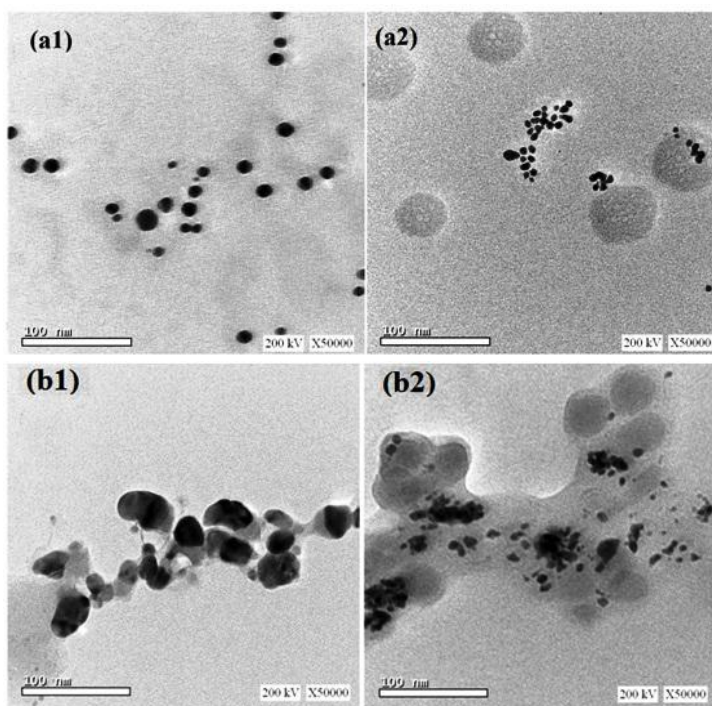
The pH of the extract used in the biosynthesis of nanoparticles is a critical factor affecting the size, shape and composition of the nanoparticles (Singh M et al., 2009). With the help of UV-vis spectroscopy and TEM analysis, the impact of Gmelina leaf extract solution pH on the biosynthesis of Au, Ag and AuAg nanoparticles was investigated within the range of pH (3-10), Figure 6. It can be seen that the absorbance increases with increasing pH from 3 to 10 with a blue shift in the spectra. Furthermore, the particles formed in the acidic medium were unstable and precipitated within 12 h while the particles prepared at pH 9 were stable for one week.





**Figure 6:** UV-Vis spectra of ( a) AuNPs (b) AgNPs (c) AuAgNPs . formed using different pH of Gmelina extract

The size of the AuNPs was followed by measuring TEM at pH5 and pH 9, Figure 7. These results were consistent with several studies which reported that at low pH, the gold nanoparticles prefer to aggregate to form larger nanoparticles rather than to nucleate and form new nanoparticles (aggregation of nanoparticles is favored over the nucleation). However, higher pH facilitates the nucleation and subsequent formation of a large number of nanoparticles with a smaller diameter. Increasing the pH increase would change the electrical charges of biomolecules which might affect their capping and stabilizing abilities and subsequently the growth of the nanoparticles (Veerasamy Ret al., 2011).



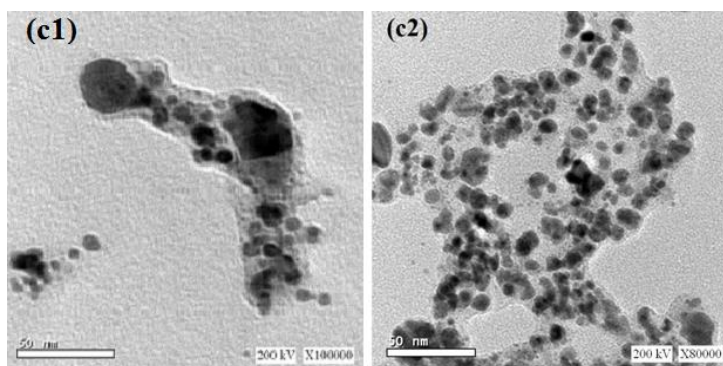


Figure 7 : TEM images of (a1)AuNPs at pH 4.5 (a2) AuNPs at pH 9 (b1) AgNPs at pH 5 (b2)AgNPs at pH 9 (c1) AuAgNPs at pH 4.2 (c2) AuAgNPs at pH 9.

It can be seen that absorbance increases with increasing pH to 8. In previous studies, it was shown that the size and shape of biosynthesized nanoparticles could be manipulated by varying the pH of the reaction mixtures. A major influence of the reaction pH is its ability to change the electrical charges of biomolecules which might affect their capping and stabilizing abilities and subsequently the growth of the nanoparticles. This result was confirmed by the TEM measurement carried out at pH 5.5 and pH 9, the size and shape of Au AgNPs were affected by changing the pH of the reaction medium. The size of the AuNps were with the average size 15 nm at pH 5.5 while at pH 9, smaller size in the range of 8 nm were found with different morphologies. The decrease in the nanoparticles size was also observed for AgNPs and AgAuNps, Figure 7.

### 3.2. X-Ray diffraction study:

X-ray diffraction data provides information about crystallinity, crystallite size, orientation of the crystallites and phase composition and aid in molecular modeling to determine the structure of the material (Joshi R et al., 2008). Advantages of XRD are the simplicity of sample preparation, rapidity of measurement, analyze mixed phases and determine sample purity. Its limitations are a requirement of homogenous and powdered material, peak overlays lead to unclear data. The green-synthesized nanoparticle was clearly analyzed using XRD measurements. Fig. 8 shows the XRD patterns of the formed nanoparticles Au, Ag and AgAuNps, respectively. The XRD patterns of Au, Ag and Ag NPs (Fig. 8) show four peaks of (1 1 1), (2 0 0), (2 2 0), (3 1 1) and (2 2 2) facets of face-centered cubic crystal structure. The broadening of Bragg's peaks indicates the formation of nanoparticles. The unknown peaks marked with x, Fig 8 b and c, could be due to crystalline bioorganic compounds from the extract.

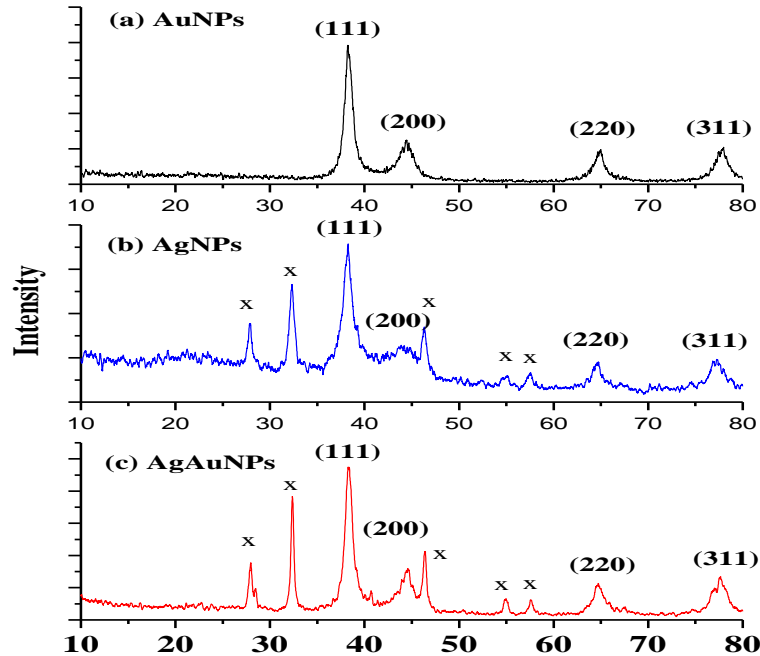


Figure.8: X-Ray diffraction patterns of (a) AuNPs and (b) AgNPs (c)AuAg prepared with aqueous *Gmelina* leaf extract.

### 3.6 Fourier transform infra-red spectroscopy (FTIR):

FTIR spectrum was used to identify the possible function groups of biomolecules in the *Gmelina* leaf extract that might be responsible for bioreduction and coating of AuNPs, AgNPs, and AgAuNPs, Fig 9. The spectrum of the FTIR spectra of *Gmelina* leaf extract showed a broad band at  $3408\text{ cm}^{-1}$ . This band attributed to the OH groups in the biomolecules. The IR bands at  $2920$  and  $2852\text{ cm}^{-1}$  due to C–H stretching vibration modes in hydrocarbon chains. The IR bands at  $1381$  and  $1732\text{ cm}^{-1}$  were characterized as C–O and C=O stretching modes of the carbonyl functional group. The stronger band at  $1642\text{ cm}^{-1}$  was characterized as C=O of the amide groups of protein in plant,  $1516\text{ cm}^{-1}$  due to stretching vibrations of –C–C– in aromatic rings. Medium bands at  $1069\text{ cm}^{-1}$  due to the C–O–C and C–OH vibrations are observed. These assignments were consisting with the isolated flavonoids as luteolin, kaempferol, isoquercitrin, quercetin-3-*O*-robinobioside from *Gmelina* extract using 90% methanol by Ghareeb et. al (GhareebM.A et al., 2014). The FTIR of AuNPs showed a shift in the absorbance peaks from  $3408.4$  to  $3412.00\text{ cm}^{-1}$  and from  $1732$  to  $1713$  and from  $1652.5$  to  $1623.0\text{ cm}^{-1}$  and  $1382.2$  to  $1419.5\text{ cm}^{-1}$ . In the case of Ag NPs, a large shift in the absorbance peak with decreased band intensity was observed from  $3408.4$  to  $3404.7\text{ cm}^{-1}$  and  $1382.2$  to  $1320\text{ cm}^{-1}$ . The spectra also illustrate a prominent shift in the wave numbers corresponding to amide ( $1652.5$ – $1600\text{ cm}^{-1}$ ), validates that free amino ( $\text{NH}_2$ ) groups in compounds of the *Gmelina* leaf extract have interacted with AgNPs surface

making AgNPs highly stable. Similar shifts were observed in the IR spectrum of AuAgNPs, the IR spectrum, Fig 9(d) indicating the capping of the nanoparticles with the extract constituents.

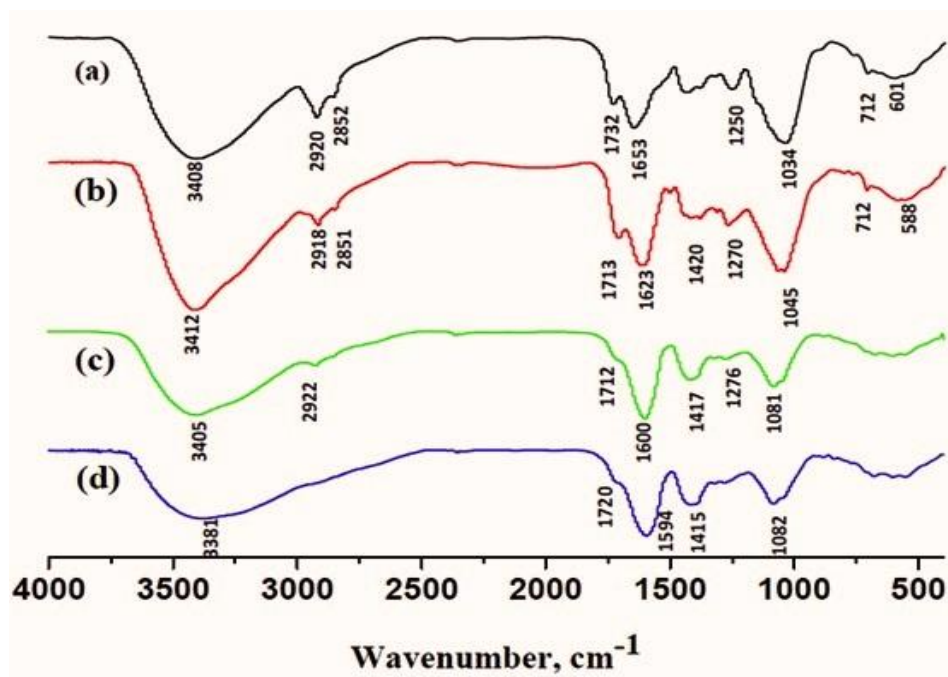


Figure 9: FTIR spectra of (A) *Gmelina* leaf extract (B) gold nanoparticles (C) silver nanoparticles (D) gold-silver nanoparticles.

### 3.7 Thermal gravimetric analysis (TGA):

The TGA plot of the capped AuNPs, capped AgNPs and AuAgNPs prepared using *Gmelina* leaf extract Fig. 11(a,b,c) showed a steady weight loss in the temperature range of 40-650 nm depending on the nanoparticles type. The amount of extract molecules present along with AuNPs, AgNPs and AuAgNPs was calculated by TGA (Fig. 10). The figure indicates that the weight loss takes place in three regions in the case of AuNPs. The first region appears around 200 °C (~10% weight loss) and the second region being around 340 °C (~35% weight loss) and the third region around 500 °C (~30% weight loss) thus corresponding to total weight loss of 75%. In case of AgNPs, the weight loss also occurs in four regions, the first at 200 °C (~15% weight loss), the second at around 335 °C (~30% weight loss), the third region at around 520 °C (~25% weight loss), and the fourth region around 600 °C giving a total weight loss of 76%. In case of AuAgNPs, the weight loss occurs also in four regions, the first around 200 °C (~14% weight loss), the second at around 335 °C (~26% weight loss), the third region at around 590 °C (~20% weight loss), and fourth region around 620 °C (~7% weight loss) giving a total weight loss of 67%. These data suggest that the AuAgNPs are more thermally stable than AuNPs and AgNPs.

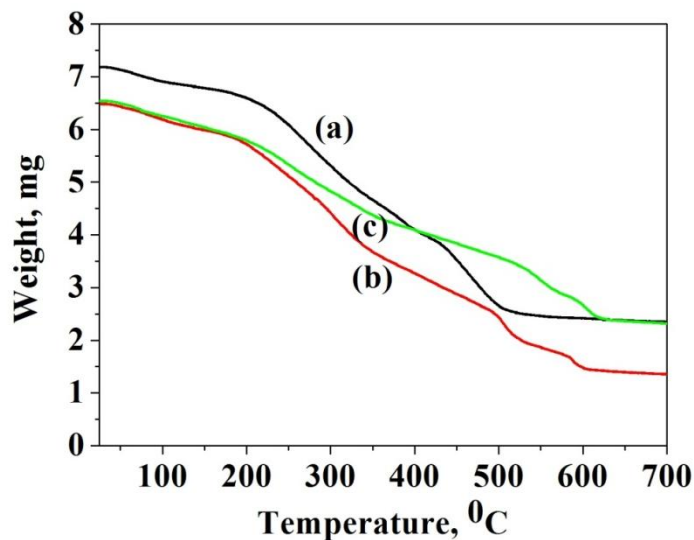


Figure10: TGA of (a) capped AuNPs using Gmelina leaf extract (b) capped AgNPs, (c)AuAgNPs.

### 3.5 Cytotoxicity Activity

Liver cancer is the third most common cause of death in cancer. The death rate is increasing and 85% people are affected in developing countries, more commonly men (SiegelR et al., 2013). Actually, *in vitro* cytotoxicity assays are widely used to chemicals including cancerchemotherapeutics, pharmaceuticals, biomaterials, natural toxins, antimicrobial agents and industrial chemicals because they are rapid and economical. These cytotoxicity tests measure the concentration of the substance that damages components, structures or cellular biochemical pathways, and they also allow direct extrapolation of quantitative data to similar *in vitro* situations (Cree (Ed.) I.A, 2011). The *in vitro* anticancer activity evaluation of the newly synthesized nanoparticles was carried out against human cancer cell lines hepatocellular carcinoma (HePG2) using MTT method (Dwivedi A.D and Gopal K, 2010). Doxorubicin hydrochloride is one of the most effective anticancer agents was used as a reference drug in this study. The relationship between drug concentrations and cell viability was plotted to calculate  $IC_{50}$ , the value which corresponds to the concentration required for 50% inhibition of cell viability and the data are shown in Table 1. According to the data in Table 1, the aqueous extract and the AuNps prepared using the extract are cytocompatible, while the AgNps and AuAgNps have cytotoxic activity with  $IC_{50}$  of 11.4 and 2.98  $\mu\text{g/ml}$  that is considered to be promising cytotoxic compared to the reference Doxorubicin. (Singh S. et al., 2010) evaluated cytotoxic and genotoxic of glycolipid-conjugated silver and gold nanoparticles on HePG2 cells. They found that both nanoparticles are found to be cytocompatible up to 100 mM metal concentrations and the gold nanoparticles are more cytocompatible than the same concentrations of silver nanoparticles. Particle size (Pan Y. et al., 2007), surface modification, type of ligand for modification, charge of the nanoparticles (Goodman C.M et al., 2004) are important parameters that control binding to cytotoxicity. It should be mentioned that the cytotoxic activity using HepG-2 assay for the pure flavonoids

(luteolin, kaempferol, isoquercitrin, quercetin-3-*O*-robinobioside)isolated from *Gmelinaarborea*Roxbshowed that the tested compounds havecytotoxic activity with IC<sub>50</sub> ranged from 3.38 to 15.70 µg/ml(**Ghareeb M. A et al., 2014**).

Table 1. Cytotoxicity (IC<sub>50</sub>) of aqueous extract of Gmelina and the nanoparticles

Item	IC <sub>50</sub> / µg
Gmelina	>50
GmelinaAuNps	>50
GmelinaAgNps	11.4
GmelinaAuAgNps	2.98
Doxorubicin HCl	1.2

### 3.6. Antimicrobial assay:

Two concentrations of *Gmelina* leaf extract were prepared 4% and 20% as used for all experiments . These stock solutions were used to prepare different solutions for the study of the antimicrobial activity of *Gmelina* leaf extract and the nanoparticles. First, two concentrations of *Gmelina* leaf extract (a1; 0.8% w/v a2 ; 4% w/v) were prepared by dilution and examined in comparison with that of newly formed nanoparticles solutions synthesized using the same *Gmelina* leaf extract concentrations (b2 & b3), The results of the antimicrobial assay were shown in Fig. 11 . Samples of *Gmelina* leaves extract at concentrations of 4 % w/v, respectively have no antimicrobial activity against all tested strains. Also, sample b2 with extract concentrations 4% w/v and Au<sup>3+</sup> (1.45X10<sup>-3</sup> M ) showed no antimicrobial activity. However, increasing Au<sup>3+</sup> concentration in sample b3 (2.9X10<sup>-3</sup> M M HAuCl<sub>4</sub>), the prepared AuNps showed antimicrobial activity against *Bacillus subtilis*, *E.coli*, *Pseudomonas aeruginosa* and *A.niger*. This activity may be due to the increase in the yield of the capped AuNPs. It is believed that due to their large surface area, nanoparticles have more penetration power into microorganisms and if the active constituents of the plant extract can be delivered to the interior of the microbes higher antimicrobial activity could be recorded(**Kvitek L. et al., 2014**).

Silver ions, as well as AgNps, were known to have strong antimicrobial activities( **Furno F et al., 2004**). The antibacterial activity of different solutions synthesized using 4% w/v plant extract added to different Ag<sup>+</sup> concentrations (c 2, 5X10<sup>-4</sup> M Ag<sup>+</sup> ) and(c3, 1X0<sup>-3</sup>M Ag<sup>+</sup>) demonstrated that AgNPs has antibacterial activity against both Gram positive and Gram negative bacteria, and the results are depicted in Figs.11. These results agreed with previous work ( **Kim J.S et al., 2007; Bindhu M.R and Umadevi M ,2013**), the activity of these solutions was mainly due to the different amounts of AgNps formed upon addition of different concentrations of *Gemlina* extract. The Gram-negative bacteria *E. coli* was less sensitive to AgNps compared with *S.aureus*. This may

be due to the characteristics of certain bacterial species (Bindhu M.R and Umadevi M, 2013). The difference in sensitivity of Gram-positive and Gram-negative bacteria to AgNPs was due to the difference in thickness (Gram positive is 50% higher than Gram-negative) and constituents of their cell membrane structure (Kim J.S et al., 2007) thus, large doses are required for Gram-positive bacteria. As well as antibacterial activity of different solutions synthesized using 4% w/v plant extract added to different Ag<sup>+</sup> and Au<sup>3+</sup> concentrations (d2, 1.45 X10<sup>-3</sup>M Au<sup>3+</sup> + 2.5X10<sup>-3</sup>M Ag<sup>+</sup>) and (d3, 2.9 x10<sup>-3</sup>M Au<sup>3+</sup> + 2.5x10<sup>-3</sup>M Ag<sup>+</sup>) demonstrated that AgAuNPs has antibacterial activity against both Gram positive and Gram negative bacteria

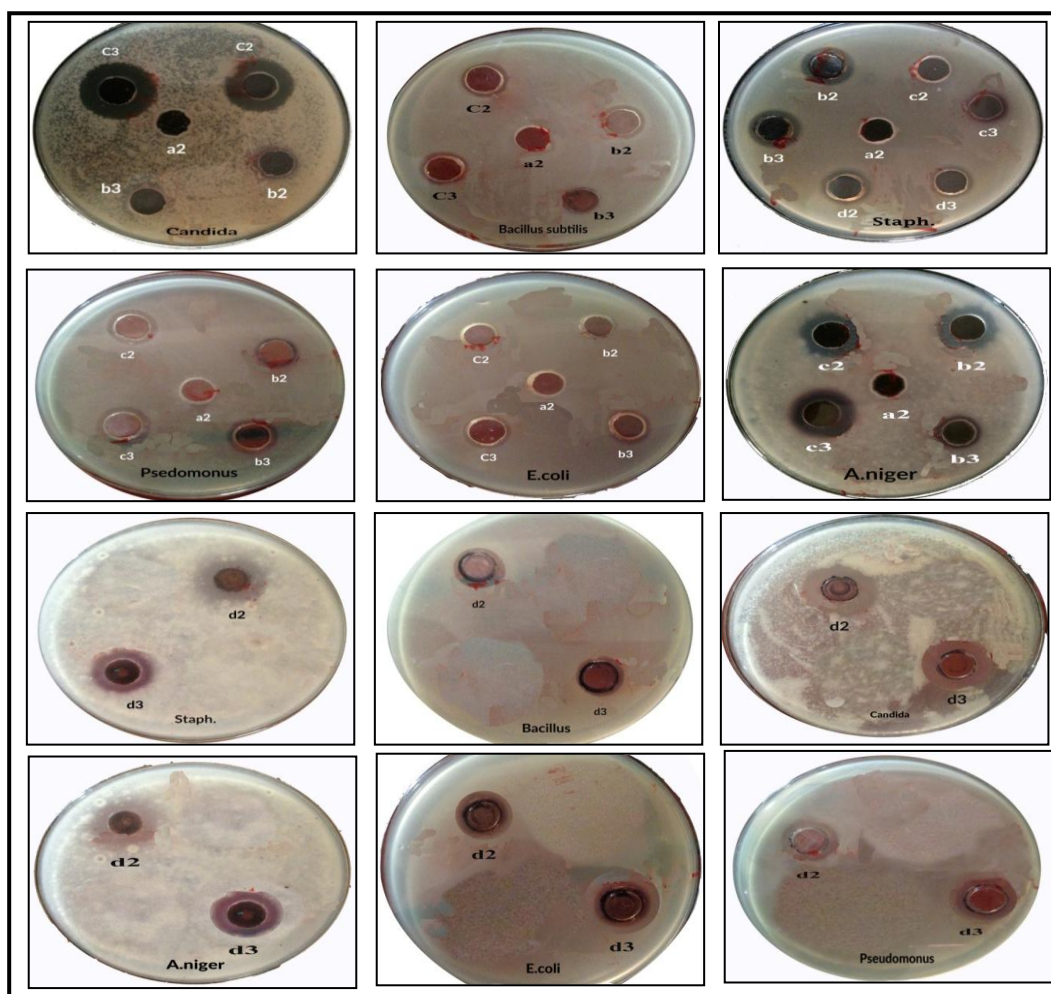


Figure 11 Antimicrobial activities of different concentrations of Gmelina leaf extract, AuNPs, AgNPs and AgAuNPs against *A. niger*, *Basillusubtillus.*, *Candida*, *E. coli*, *pseudomonas.*, *Staph aureus*.



## Conclusion

This work presented synthesis consisting of a reduction of the silver and gold ions using a Gmelina leaf extract for the first time. The silver, gold and AgAu-core shell nanoparticles were characterized using different techniques. The toxicity effects of AgNps, AgNps as well as AgAu core-shell bimetallic NPs on the liver carcinoma cell line (HePG2) were examined and found that the IC<sub>50</sub> of AgAuNps (2.98mg/ml) is higher than AgNps (11.4mg/ml) and AuNPs (>50mg/ml) or Gmelina (>50mg/ml). The antimicrobial activity of the prepared nanoparticles were studied and the activity was found to depend on the concentration of nanoparticles and their sizes.

## REFERENCES

- Ahmed S.**, Annu, S.Ikram, S.Yudha, Biosynthesis of gold nanoparticles: A green approach *J. Photochem. Photobiol. B: Biology*, 161 141-153 (2016).
- Atta AM**, GA El-Mahdy, HA Al-Lohedan, AO Ezzat, Preparation of crosslinked amphiphilic silver nanogel as thin film corrosion protective layer for steel. *Molecules*. 19 10410–10426 (2014).
- Bindhu M.R.**, M. Umadevi, Synthesis of monodispersed silver nanoparticles using Hibiscus cannabinus leaf extract and its antimicrobial activity, *SpectrochimicaActa Part A* 101 184–190 (2013).
- Cederquist K. B.**, B. Liu, M. R. Grima, P. J. Dalack, J. T. Mahorn, Laser-fabricated gold nanoparticles for lateral flow immunoassays, *Colloids and Surfaces B: Biointerfaces* 149 351-357 (2017).
- Chandran S.P.**, M.Chaudhary, R.Pasricha, A.Ahmad, M.Sastry., Synthesis of gold nanotriangles and silver nanoparticles using Aloe Vera plant extract. *Biotechnol. Prog.* 22 577–588 (2006).
- Chen H.M.**, R.S. Liu, L.-Y.Jang, J.-F. Lee, S.F. Hu Characterization of core–shell type and alloy Ag/Au bimetallic clusters by using extended X-ray absorption fine structure spectroscopy *Chemical Physics Letters* 421 118–123 (2006).
- Cho J-H**, A-Ru Kim, S. Kim, S. Lee, H. Chung, M. Yoon, Development of a novel imaging agent using peptide-coated gold nanoparticles toward brain glioma stem cell marker CD133 *Acta Biomaterialia*, 47, 182-192 (2017).
- Cree (Ed.) I. A.**, Cancer Cell Culture: Methods and Protocols, Second Edition *Methods in Molecular Biology*, 731, Springer Science+Business Media, LLC (2011).
- Das VL**, R Thomas, RT Varghese, EV Soniya, J Mathew, EK. Radhakrishnan, Extracellular synthesis of silver nanoparticles by the *Bacillus* strain CS 11 isolated from industrialized area. *Biotech.* 4 121–126 (2014).
- Dwivedi A.D. and K. Gopal, Biosynthesis of silver and gold nanoparticles using *henopodium album* leaf extract *Colloids and Surfaces A*, 369 27–33 (2010).
- Furno F.**, KS Morley, B, Wong et al. Silver nanoparticles and polymeric medical devices: a new approach to prevention of infection? *J Antimicrob. Chemother.* 54 1019–1024(2004).

- Galdiero S.**, A.Falanga,;M. Vitiello, M. Cantisani, V.Marra, M. Galdiero, Silver nanoparticles as potential antiviral agents. *Molecules*16 8894-8918 (2011).
- Ghareeb M. A.**, H. A. Shoeb, H. M.F. Madkour,L. A. Refahy, M. A. Mohamed and A. M. Saad, Antioxidant and Cytotoxic Activities of Flavonoidal Compounds from *Gmelina arborea* RoxbGlobal Journal of Pharmacology 8 (1): 87-97, (2014).
- Ghosh S.**, S. Patil, M. Ahire, R. Kitture, S. Kale, K. Pardesi, S. S Cameotra, J. Bellare, D. D Dhavale, A. Jabgunde, B. A Chopade, Synthesis of silver nanoparticles using *Dioscoreabulbiferatuber* extract and evaluation of its synergistic potential in combination with antimicrobial agents. *Int J Nanomedicine*. 7 483–496 (2012).
- Goodman C. M.**, C. D. McCusker, T. Yilmaz and V. M. Rotello, Toxicity of gold nanoparticles functionalized with cationic and anionic side chains, *Bioconjugate Chem.*, , 15, 897–900 (2004).
- Huang S. H.** Gold nanoparticle-based immunochromatographic test for identification of *Staphylococcus aureus* from clinical specimens, *Clin. Chim.Acta* 373- 139 (2006).
- Jagtap U.B.**, VA Bapat. Green synthesis of silver nanoparticles using *Artocarpus Heterophyllus* Lam. seed extract and its antibacterial activity. *Ind Crops Prod*. 46 132–137 (2013).
- Joshi M**, Bhattacharyya A, Ali SW, Characterization techniques for nanotechnology applications in textiles, *Indian journal of fiber & textile research*, 33 304–317(2008).
- Kampa M.**, A. Hatzoglou, G. Notas, A. Damianaki, E. Bakogeorgou, C. Gemetzi, E. Kouroumalis, PM Martin, E. Castanas Wine antioxidant polyphenols inhibit proliferation of human prostate cancer cell lines. *Nutr Cancer*. 37 223-33(2000) .
- Kaswala R.** , V. Patel, Chakraborty M, Kamath JV. Phytochemical and pharmacological profile of *Gmelinaarborea*: An overview. *Int Res J Pharm*.3 61-64 (2012) .
- Khali M.M.H.** I, EH Ismail, KZ El-Baghdady, D. Mohamed, Green synthesis of silver nanoparticles using olive leaf extract and its antibacterial activity. *Arab J Chem*. 71131–1139 (2014).
- Khali M.M.H.** I, E. H. Ismail, F. El-Magdoub Biosynthesis of Au nanoparticles using olive leaf extract *Arabian Journal of Chemistry* 5 431–437(2012)
- Kim J.S.**, , E. Kuk, ,K.N. Yu, J.-H. Kim, S.J. Park, H.J Lee., S.H. Kim, Y.K. Park, Y.H. Park, C.-Y Hwang., Y.-K Kim., Y.-S. Lee, D.H. Jeong, M.-H. Cho., Antimicrobial effects of silver nanoparticles, *Nanomed. Nanotechnol. Biol. Med*. 3 95–101 (2007).
- Lara H.H;** N.V. Ayala-Nuñez, L.Ixtepan-Turrent, C. Rodriguez-Padilla, Mode of antiviralaction of silver nanoparticles against HIV-1. *J. Nanobiotechnol* 8. 1–10 (2010).
- Li W.R.**, , X.B Xie., , Q.S. Shi, H.Y. Zeng, Y.S. Ou-Yang, ,Y.B. Chen, Antibacterial activity and mechanism of silver nanoparticles on *Escherichia coli*. *Appl. Microbiol. Biotechnol*. 85 1115–1122 (2010).
- Li Y.**, P. Leung, L.Yao, Q. Song, E. Newton, Antimicrobial effect of surgical masks coated with nanoparticles. *J Hosp Infect*. 62 58–63(2006).

- Lu.Z.**, KRong, JLi, H. Yang, R.Chen, Size-dependent antibacterial activities of silver nanoparticles against oral anaerobic pathogenic bacteria. *J Mater Sci Mater Med.* 24 1465–1471(2013)
- Lukianova-Hleb E.Y.**, D.S. Wagner, M.K. Brenner, D.O. Lapotko, Cell-specific transmembrane injection of molecular cargo with gold nanoparticle-generated transient plasmonic nanobubbles *Biomaterials*, 33 5441-5450 (2012) .
- Mallik K.**, M. Mandal, N. Pradhan, T. Pal, Seed Mediated Formation of Bimetallic Nanoparticles by UV Irradiation: A Photochemical Approach for the Preparation of “Core-Shell” Type Structures *NanoLetters* 1 319(2001).
- Mecha CA**, VL Pillay, Development and evaluation of woven fabric microfiltration membranes impregnated with silver nanoparticles for potable water treatment. *J Memb Sci.* 458 149–156 (2014).
- Mittal A.K.** , Y. Chisti, U.C. Banerjee. Synthesis of metallic nanoparticles using plant extracts. *Biotech Adv.* 31 346–356 (2013).
- Murphy C.J**, A.M. Gole, J.W. Stone, P.N. Sisco, A.M. Alkilany, E.C. Goldsmith, S.C. Baxter, Gold nanoparticles in biology: beyond toxicity to cellular imaging *Acc. Chem. Res.*41 1721–1730 (2008).
- Noruzi M. Biosynthesis of gold nanoparticles using plant extracts *Bioprocess Biosyst Eng.*38 1–14(2015).
- Oprisa R.**, C. Tatomirb, D. Olteanu, R. Moldovan, B. Moldovanc, L. David, A. Nagy, N. Deceaa, M. L. Kiss, G. A. Filip The effect of *Sambucus nigra* L. extract and phytothesized gold nanoparticles on diabetic rats *Colloids and Surfaces B: Biointerfaces* 150 192–200 (2017).
- Pal S. Y.K.** Tak, JM.Song, Does the antibacterial activity of silver nanoparticles depend on the shape of the nanoparticle? A study of the Gram-negative bacterium *Escherichia coli*. *Appl Environ Microbiol.* 73(6) 1712–1720 (2007)
- Pan Y.**, S. Neuss, A. Leifert, M. Fischler, F. Wen, U. Simon, G. Schmid, W. Brandau and W. Jahnen-Dechent, *Small*, 3 1941–1949 (2007).
- Pradeepa K ,U.Bhat, S.M. Vidya, Nisingold nanoparticles assemble as potent antimicrobial agent against *Enterococcus faecalis* and *Staphylococcus aureus* clinical isolates *J. Drug Deliv. Sci. Technol.*, 37 20-27(2017).
- Prabhu S.**, EK.Poulose, Silver nanoparticles: mechanism of antimicrobial action, synthesis, medical applications, and toxicity effects. *Int NanoLett.* 2 1–10 (2012)
- Qin L**, G. Zeng, C. Lai, D. Huang, C. Zhang, P. Xu, T. Hu, X. Liu, M. Cheng, Y. Liu, L. Hu, Y. Zhou, A visual application of gold nanoparticles: Simple, reliable and sensitive detection of kanamycin based on hydrogen-bonding recognition *Sensors and Actuators B* 243 946–954 (2017).

**Rajan A.A.**, R.Rajan, D. Philip *Elettaria cardamomum* seed mediated rapid synthesis of gold nanoparticles and its biological activities *OpenNano2* 1–8 (2017).

Shankar S. S., A. Rai, A., Ahmad and M. Sastry, Rapid synthesis of Au, Ag, and bimetallic Au core-Ag shell nanoparticles using Neem (*Azadirachta indica*) leaf broth *J. Colloid Interf. Sci.*, 275 496 (2004).

**Siddiqi K.S.**, A.Husen, Recent advances in plant-mediated engineered gold nanoparticles and their application in biological system *Journal of Trace Elements in Medicine and Biology* 40 10–23(2017).

**Singh M.**, I. Sinha, R.K. Mandal Role of pH in the green synthesis of silver nanoparticles *Materials Letters* 63425–427(2009).

**Singh S.**, V. D'Britto, A. A. Prabhune, C. V. Ramana, A. Dhawan and B. L. V. Prasad, Cytotoxic and genotoxic assessment of glycolipid-reduced and –capped gold and silver nanoparticles *New J. Chem* 34 294–301(2010).

**Skehan P.**, R. Storeng, D. Scudiero, A. Monks, J. McMahon, D. Vistica, J.T. Warren, H. Bokesch, S. Kenney and M.R. Boyd, J. McMahon, D. Vistica,. New colorimetric cytotoxicity assay for anticancer-drug screening. *Food Chem.Toxicol.* 34449-56 (1996).

**Song J. Y.** , B.S Kim Biological synthesis of bimetallic Au/Ag nanoparticles using Persimmon (*Diopyros kaki*) leaf extract *Korean J. Chem. Eng.*, 25(4) 808-811(2008).

**Sperling R.A.** , Gil, P.R., Zhang, F., Zanella, M., Parak, W.J., Biological applications of gold nanoparticles. *Chem. Soc. Rev.* 37 1896–1908 (2008) .

**Sun Y.**, B. T. Mayers, Y. Xia Template-Engaged Replacement Reaction: A One-Step Approach to the Large-Scale Synthesis of Metal Nanostructures with Hollow Interiors *Nano Lett.*, 2 481(2002).

**Syed A.**, S. Saraswati, GC Kundu, A. Ahmad, Biological synthesis of silver nanoparticles using the fungus *Humicolasp.* and evaluation of their cytotoxicity using normal and cancer cell

**Sylvie L.W.**, N. Paulin, B.N. Tèlesphore, F.K.F. Siaka, A.D. Atsamo, K. Albert, In vivo antioxidant and vasodilating activities of *Gmelina arborea* (Verbenaceae) leaves hexane extract. *Journal of complementary and Integrative Medicine.* 9(1) 26 (2012) .

**Veerasamy R.**, T.Z. Xin, S. Gunasagaran, T.F.W. Xiang, E.F.C. Yang, N. Jeyakumar, S.A Dhanaraj, Biofabrication of Ag nanoparticles using *Moringa oleifera* leaf extract and their antimicrobial activity *J. Saudi Chem. Soc.*, 15 113-120(2011) .

**Wilson R.**, The use of gold nanoparticles in diagnostics and detection. *Chem. Soc.Rev.* 37 , 2028–2045 (2008).